IEEE Transactions on Nuclear Science, Vol. NS-30, No. 4, August 1983

DEVELOPMENT OF AN RFQ LINAC AT KEK

T. Kato, Z. Igarashi, C. Kubota, E. Takasaki, T. Takenaka and S. Fukumoto
KEK, National Laboratory for High Energy Physics
Oho-machi, Tsukuba-gun, Ibaraki-ken, 305, Japan

Summary

An RFQ model linac of 62 cm long at a frequency of 200 MHz was constructed using a computer program "QKEK" developed at KEK. QKEK generates an RFQ linac, calculates beam dynamics, and provides geometrical data of vanes for a numerically controlled milling machine. A detailed study of rf characteristics was performed. The accelerating and focusing fields measured by the bead perturbation method on axis agree well with the design values. An RFQ linac, which accelerates protons from 50 keV to 750 keV, is designed.

Introduction

One of problems of the RFQ linac mechanical design is how to mount vanes to the cavity. The four vanes, which generate accelerating and focusing rf fields on axis, must be assembled to the cavity with mechanical precision keeping good electric contact. In LANL, sophisticated structures have been used to tune the vane position mechanically.[1] If, however, the cavity is rectangular instead of cylindrical, then alignment of the vanes becomes much simpler and it is possible to weld all contacts of the cavity by electron beam assuring high conductivity. The Q-values were calculated by SUPERFISH in a circular and rectangular cross-sectional cavity. In a rectangular cavity Q_0 of 12725 was obtained, while Q_0 was 12676 in a circular one.

Cold model linac

A model linac of 62 cm long (Fig. 1), made of aluminum except for the vane poles, was constructed considering application to a hot RFQ linac. A lot of cavity components of different type were prepared to study rf characteristics of the model cavity. They were fastened to the cavity with screws. The parameters of the model linac are summarized in Table 1. Although this model linac is shorter than the planned hot one, it contains three different structures: the matching, bunching, and accelerating sections. Accelerating field increases linearly with distance in order to facilitate the comparison between measurement and theory (Fig. 2).

Three kinds of the vane pole were prepared. The first is the straight vane with the pole tip radius of 6 mm. The second is with 5 mm radius and the third is a set of modulated vanes.

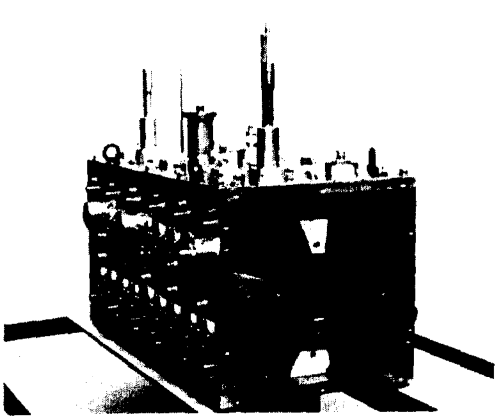

Fig. 1 Photograph of the model linac.

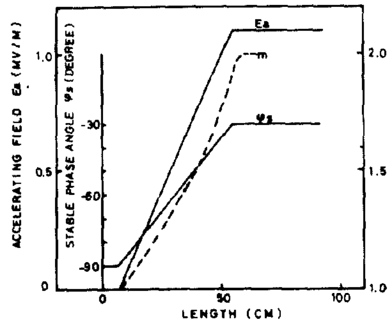

Fig. 2 Parameters of the model linac.

Table 1 Parameters of the cold and hot linac

	cold model	hot model	
Frequency	201.08	201.08	MHz
Injection energy	50	50	keV
Final energy	153	750	keV
Vane voltage	22	89	kV
Number of cells	66	118	
Vane length (L)	59.5	136.4	cm
Initial radius	2.3	2.4	cm
Minimum radius	0.4	0.4	cm
Initial modulation	1.0	1.0	
Maximum modulation	2.0	2.0	
Initial phase	-90.0	-90.0	
Final phase	-30.0	-30.0	
Normalized Acceptance		0.41	π cm·mrad

Machining of vanes

The most important part of an RFQ linac, modulated vanes, were machined precisely by a numerical controlled (NC) milling machine in the KEK machine shop. It took 39 hours to machine a vane of 59 cm long, thus a change of temperature and the accumulative errors of the NC machine itself could not be ignored. Then we measured the motion of the NC machine by three magnetic scales and compensated the error within ± 25 μm during machining. Generation of the vane geometry by the computer program QKEK is described in ref. 2.

Resonant frequency measurement

The resonant frequencies measured are given in Table 2. The fundamental frequencies of TE210 and TE110-like modes are separated sufficiently to avoid the excitation of both at the same time.

Since the average pole tip radius of the modulated vanes was not designed to be constant, it was approximated considering the modulated capacitance between the adjacent vanes as:

$$r = \frac{1}{\sqrt{2}L} \int_0^L (r_x(z)^2 + r_y(Z)^2)^{1/2} dz \quad , \qquad (1)$$

where $r_x(z)$ and $r_y(z)$ are radii of two kinds of vanes. The TE210-like mode frequencies agree with the results of SUPERFISH within 0.9%.

Table 2 Resonant frequencies of three types of vanes

Vane type	Measured values TE210 f_0 (MHz)	TE110 f_{01}	f_{02}	FISH results TE210
5 mm	198.4	218.6	221.1	197.208
6 mm	209.1	218.5	219.5	207.461
modulated	211.1	218.6	221.1	209.311

Axial field measurement

The bead perturbation method was used for measuring the axial fields. Self-excited oscillator was employed for this measurement. The measurements were done automatically using a personal computer except for driving a bead. The drift of the resonant frequency during five minutes was within 10 Hz, while a change of the resonant frequency due to the perturbation was more or less 1000 Hz. An aluminum bead (2 mm in diameter and 3 mm in length) was manually moved.

The perturbation formula is given by[3]:

$$\omega^2 = \omega_0^2(1 + \int(H^2 - E^2)dv) \quad , \tag{2}$$

where ω_0 is the unperturbed angular frequency, ω is the perturbed frequency.

Since the variation of the electric field in the volume of the bead can not be ignored, all componets of the field should be taken into account. Supposing that there is no magnetic field in the space among vane poles and the bead is on the axis, the results are given by:

$$\Delta\omega \propto -(I_r + I_\phi + I_z) \quad , \tag{3}$$

$$\begin{aligned} I_r' &= \int E_r^2 \, dv \\ &= \frac{(XV)^2}{a^4}\frac{r_0^4}{4}\pi\ell + \frac{(kAV)^2}{4} \, 2\pi \, \frac{k^2 r_0^2}{16} r_0^2 \\ &\quad \times \left(\frac{\ell}{2} + \frac{1}{2k}\sin k\ell \, \cos 2kz_0\right) \quad , \end{aligned} \tag{4}$$

$$I_\phi = \int E_\phi^2 \, dv = \frac{(XV)^2}{a^4}\frac{r_0^2}{4}\pi\ell \quad , \tag{5}$$

$$\begin{aligned} I_z &= \int E_z^2 \, dv \\ &= \frac{(kAV)^2}{4} \, 2\pi \, \frac{r_0^2}{2}\left(\frac{\ell}{2} - \frac{1}{2k}\sin k\ell \, \cos 2kz_0\right) \quad , \end{aligned} \tag{6}$$

where ℓ and r_0 represent length and radius of the bead, respectively. The formulas of the electric fields in an RFQ linac used in the equations above are similar to those in ref. 4.

The perturbation signals obtained in the end part of the modulated vane are shown in Fig. 3. Figure 4 shows the fine structure of the signals. The calculated values using eq. (3) are shown in the solid line. The values considering only E_z term are shown in the dashed line. Figure 5 shows the distribution of the electric fields along the axis. The signals from the matching section and the bunching section are shown in Fig. 6 and Fig. 7.

The azimuthal field was also measured by the bead perturbation method with an aluminum sphere of 4 mm in diameter. The designed azimuthal field was obtained in the region of vane tip approximated by a part of a circle.

It is concluded from these measurements that the desirable accelerating field can be realized satisfactorily by modulation of vanes.

A planned RFQ linac

Both polarized protons and H^- beam injection into the Booster Synchrotron are scheduled in the near future at KEK. The beam intensity of the polarized protons ($\sim$ 10 μA) is smaller than the proton beam intensity by four orders of magnitude and that of the H^- beam ($\sim$ 10 mA) by one order. Therefore an RFQ linac, whose maximum current is limited by space charge to the rather small value, is suitable for the acceleration of both beams.

On the basis of the cold model study, an RFQ linac of rectangular cross section (Fig. 8) was designed. Design parameters are summarized in Table 1. Several beam dynamics calculations in the linac are shown in Figs. 9-11. The four vanes are under construction.

Acknowledgements

The authors would like to thank Dr. D.A. Swenson and Dr. S.O. Schriber for many helpful discussions during their stays at KEK.

References

1. L.D. Hansborough, J.M. Potler and N.G. Wilson, Proc. of 1981 Linac Conf., 329 (1981).
2. T. Kato et al., to be published in KEK report.
3. J.C. Slator, Microwave Electronics (D.Van Nostrand Company, Inc., New York, 1950), p.81.
4. K.R. Crandall, R.H. Stokes, and T.P. Wangler, Proc. of 1979 Linac Conf., 205 (1979).

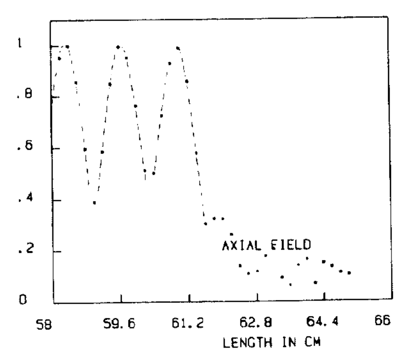

Fig. 3 Typical signals on the axial perturbation in the end part of the modulated vanes. Length on abscissa is measured from the input end plate.

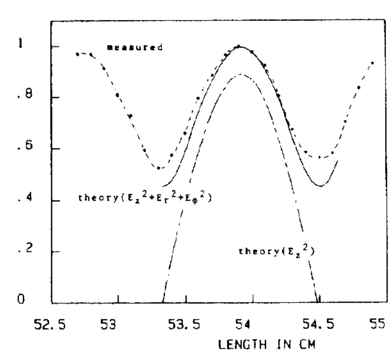

Fig. 4 Fine structures of the signals on the axial perturbation.

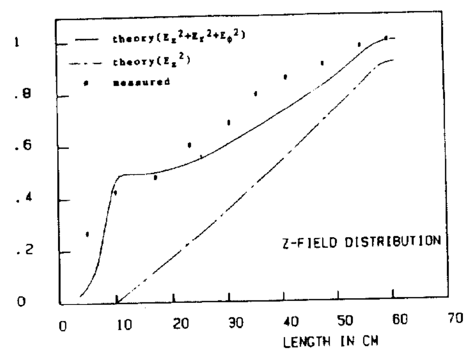

Fig. 5 Distribution of the axial fields in the linac.

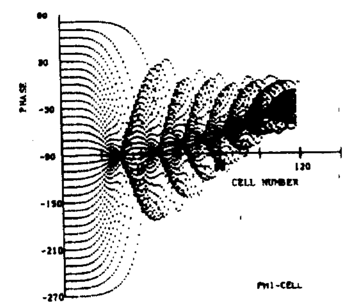

Fig. 11 Phase oscillation in the RFQ linac.

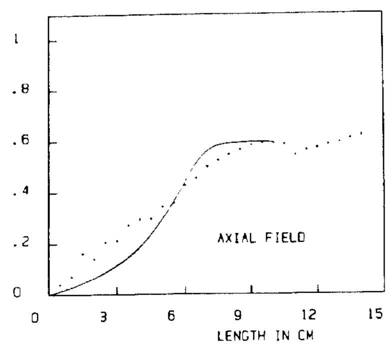

Fig. 6 Signals on the axial perturbation in the matching section. The solid line shows the results of calculation using E_r, E_ϕ and E_z.

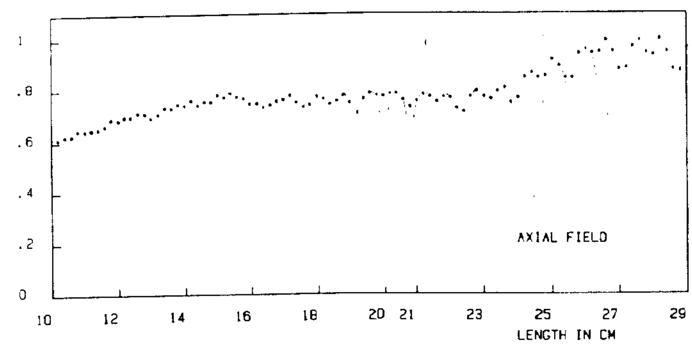

Fig. 7 Signals on the axial perturbation in the bunching section.

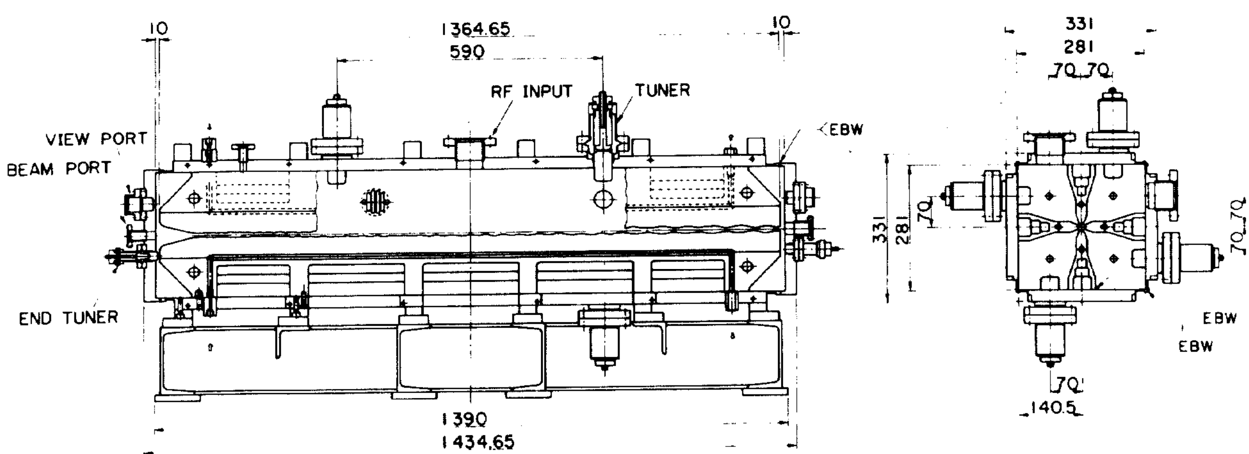

Fig. 8 Planned 750 keV RFQ linac.

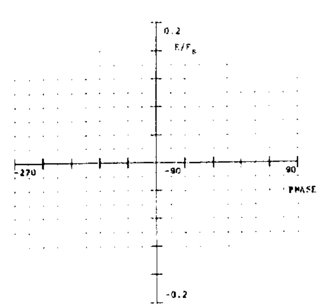

Fig. 9 Longitudinal acceptance at entrance of the RFQ linac. E_s is the energy of the phase stable particle.

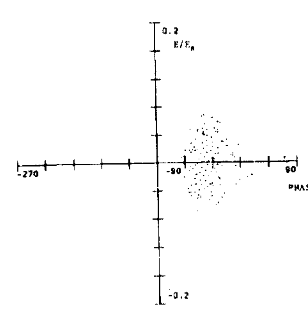

Fig. 10 Longitudinal emittance at exit of the RFQ linac. E_s is the energy of the phase stable particle.